



eCOMMONS

Loyola University Chicago
Loyola eCommons

Biology: Faculty Publications and Other Works

Faculty Publications

5-2015

Using Whole-Genome Sequences of the LG/J and SM/J Inbred Mouse Strains to Prioritize Quantitative Trait Genes and Nucleotides

Igor Nikolskiy

Donald F. Conrad

Sung Chun

Justin C. Fay

James M. Cheverud

Loyola University Chicago, jcheverud@luc.edu

See next page for additional authors

Recommended Citation

Nikolskiy, Igor; Conrad, Donald F.; Chun, Sung; Fay, Justin C.; Cheverud, James M.; and Lawson, Heather A.. Using Whole-Genome Sequences of the LG/J and SM/J Inbred Mouse Strains to Prioritize Quantitative Trait Genes and Nucleotides. *BMC Genomics*, 16, 415: 1-12, 2015. Retrieved from Loyola eCommons, Biology: Faculty Publications and Other Works, <http://dx.doi.org/10.1186/s12864-015-1592-3>

This Article is brought to you for free and open access by the Faculty Publications at Loyola eCommons. It has been accepted for inclusion in Biology: Faculty Publications and Other Works by an authorized administrator of Loyola eCommons. For more information, please contact ecommons@luc.edu.



This work is licensed under a [Creative Commons Attribution 4.0 License](http://creativecommons.org/licenses/by/4.0/).

Authors

Igor Nikolskiy, Donald F. Conrad, Sung Chun, Justin C. Fay, James M. Cheverud, and Heather A. Lawson

RESEARCH ARTICLE

Open Access

Using whole-genome sequences of the LG/J and SM/J inbred mouse strains to prioritize quantitative trait genes and nucleotides

Igor Nikolskiy¹, Donald F Conrad¹, Sung Chun², Justin C Fay¹, James M Cheverud³ and Heather A Lawson^{1*}

Abstract

Background: The laboratory mouse is the most commonly used model for studying variation in complex traits relevant to human disease. Here we present the whole-genome sequences of two inbred strains, LG/J and SM/J, which are frequently used to study variation in complex traits as diverse as aging, bone-growth, adiposity, maternal behavior, and methamphetamine sensitivity.

Results: We identified small nucleotide variants (SNVs) and structural variants (SVs) in the LG/J and SM/J strains relative to the reference genome and discovered novel variants in these two strains by comparing their sequences to other mouse genomes. We find that 39% of the LG/J and SM/J genomes are identical-by-descent (IBD). We characterized amino-acid changing mutations using three algorithms: LRT, PolyPhen-2 and SIFT. We also identified polymorphisms between LG/J and SM/J that fall in regulatory regions and highly informative transcription factor binding sites (TFBS). We intersected these functional predictions with quantitative trait loci (QTL) mapped in advanced intercrosses of these two strains. We find that QTL are both over-represented in non-IBD regions and highly enriched for variants predicted to have a functional impact. Variants in QTL associated with metabolic (231 QTL identified in an F₁₆ generation) and developmental (41 QTL identified in an F₃₄ generation) traits were interrogated and we highlight candidate quantitative trait genes (QTG) and nucleotides (QTN) in a QTL on chr13 associated with variation in basal glucose levels and in a QTL on chr6 associated with variation in tibia length.

Conclusions: We show how integrating genomic sequence with QTL reduces the QTL search space and helps researchers prioritize candidate genes and nucleotides for experimental follow-up. Additionally, given the LG/J and SM/J phylogenetic context among inbred strains, these data contribute important information to the genomic landscape of the laboratory mouse.

Keywords: Mouse models, Quantitative trait loci (QTL), Complex traits, Identity-by-descent (IBD), Predicted deleterious mutations, Quantitative trait gene (QTG), Quantitative trait nucleotide (QTN), Candidate loci, Whole genome sequence, Small nucleotide variant (SNV)

Background

The LG/J (large) and SM/J (small) strains of inbred mice were independently derived from selection experiments for large and small body size at 60 days, respectively [1]. LG/J was created from a pool of albino mice obtained from a commercial breeder over a nine-month period and selected for increased body size for over 50 generations [2,3].

SM/J was created from a pool of mice derived from four crosses of seven inbred strains: dilute brown agouti (*dba*), silver chocolate (*sv ba*), black and tan (*a^t*), pink-eyed, short-eared dilute brown agouti (*ps^e dba*), albino (*c*), cinnamon spotted (*bs*), and agouti (*a*) [4]. It is unclear whether any of these strains are related to current laboratory inbred strains. The SM/J strain is kept heterozygous at the *agouti* locus by mating black animals (*a/a*) with their white-bellied agouti (*A^w/a*) siblings. Attempts to fix the SM/J strain or its Recombinant Inbred Strain offspring for the SM/J allele at *agouti* have resulted in strain failure [5].

* Correspondence: hlawson@genetics.wustl.edu

¹Department of Genetics, Washington University School of Medicine, Campus Box 8108 660 S Euclid Ave, St Louis, MO 63110, USA
Full list of author information is available at the end of the article

Subsequent to selection, the LG/J and SM/J strains are fully inbred and have been maintained at the Jackson Laboratory since the 1950s by brother-sister mating. They are at the extremes of the adult body size distribution among the common laboratory inbred strains and have been profitably studied for genetic variation in adult body size and growth [6-18]. Early genetic studies of these two strains found the differences in body size are caused by many genes of individually small effects [8]. This result has been confirmed in many quantitative trait locus (QTL) mapping studies. The strains have remained phenotypically stable over time, except that the SM/J strain is now about 6g heavier than it was in Chai's studies [19].

LG/J and SM/J differ in many complex traits in addition to size and growth. The parental strains and their crosses differ in skeletal morphology, including the size and shape of the skull [20-22], mandible [23-30], tooth morphology [31,32], long-bone lengths [33-37], and a variety of other skeletal elements as well as bone biomechanical and structural properties [38,39].

They also differ for a variety of metabolic traits including obesity, diabetes, and serum cholesterol, triglycerides, and free fatty acids levels [40-51]. The SM/J strain responds more strongly than LG/J to a high-fat diet for these metabolic traits. The two strains also differ for maternal genetic effects on offspring growth and offspring adult metabolic traits [52-56] and their cross has been useful in mapping parent-of-origin genetic effects on metabolic traits [48-51,53,57].

In addition to these diverse metabolic and skeletal phenotypes, the LG/J strain shows the rare ability to regenerate tissues after injury. The LG/J strain regenerates ear pinna tissues after a 2mm hole-punch [58-61] while the SM/J strain does not. The LG/J strain also can regenerate damaged articular cartilage [62] and is protected from post-traumatic osteoarthritis [63].

Others have mapped a variety of behavioral phenotypes using a LG x SM cross, including prepulse inhibition [64] and methamphetamine sensitivity and locomotor activity [65]. Additional studies have investigated blood cell parameters [66] and skeletal muscle weight and fiber types [67,68].

Here we describe the whole-genome sequences of the LG/J and SM/J inbred mouse strains, adding two more sequences to the collection of whole-genomes of laboratory mice [69,70]. We integrate these sequences with quantitative trait loci (QTL), and illustrate how top-down (phenotype to genomic sequence) and bottom-up (genomic sequence to phenotype) approaches can be used to identify candidate quantitative trait genes (QTG) and prioritize positional candidate quantitative trait nucleotides (QTN) for further mechanistic studies. Results from QTL studies using crosses of LG/J and SM/J will be more interpretable given these whole-genome sequences.

Results and discussion

LG/J and SM/J whole-genome sequences

Sequence was generated from DNA isolated from 1 LG/J female and 1 SM/J female as described below. Variants (comprised of small nucleotide variants (SNVs) including single nucleotide polymorphisms (SNPs) and small insertion-deletions (Indels) and structural variants (SVs) including deletions, insertions and inversions) were discovered based on whether they were the same as, or different from, the C57BL/6J reference sequence (mm10, NCBI build 38). Greater than 90% of reads for each strain could be uniquely mapped to the reference genome and, based on a genome size of 2.5G, our coverage is approximately 35X and 30X for LG/J and SM/J, respectively. Overviews of annotated variants identified for each strain individually, as well as those that are polymorphic between LG/J and SM/J, are described in Tables 1 and 2 and in Additional files 1 and 2. SNVs identified for the LG/J strain are available in Additional files 3 and 4 and for the SM/J strain in Additional files 5 and 6. Structural variant positions and classifications for each strain are available in Additional file 7. Polymorphic variants and their genomic context are illustrated in Figure 1. Quality was assessed by comparing our SNP calls with SNPs in dbSNP that were called from unpublished low-coverage sequence generated independently via two separate library preparations for LG/J ($\approx 18X$) and SM/J ($\approx 14X$) (Table 3).

We compared SNPs identified in LG/J and SM/J to those identified in other mouse strains sequenced at high coverage and identified novel variants (Table 1). Pairwise distances were calculated for LG/J and SM/J from each of these strains and a phylogenetic tree was constructed using all 20 mouse sequences (Additional files 8 and 9). The LG/J and SM/J ancestries are expected given what we know about their origins and previous studies of inbred mouse phylogenies [71]. It has been suggested that the SM/J strain may be related to the current DBA strains, DBA/1J and DBA/2J, as one of the seven strains contributing to the base population that was selected for smaller body weight was a *dba* strain named after its dilute brown agouti coat color [72]. Comparison of SNPs between LG/J or SM/J and the sequenced DBA/2J shows no specific relationship between SM/J and DBA/2J. However, the percent shared SNPs between inbred mouse strains can be biased by the use of C57BL/6J as the reference genome since variants may be missed due to alignment quality favoring bases that match the reference.

Functional predictions

Deleterious amino acid mutations in LG/J and SM/J were predicted using three independent methods: LRT [73], PolyPhen-2 [74] and SIFT [75] as implemented in VEP [76]. The LRT compares the probability that a

Table 1 Sequence and variants overview

Strain	Total reads	% Mapped to reference	Coverage	SNPs	Strain-Specific SNPs*	Indels	Strain-Specific Indels*	SVs	Strain-Specific SVs*
LG/J	9.6x10 ⁸	91.72	35X	4,663,723	146,814	1,127,072	56,469	12,802	1,361
SM/J	7.7x10 ⁸	92.67	30X	4,792,568	227,132	1,127,458	65,935	15,564	2,255

*Refers to strain-specific variants with respect to 18 other available mouse genome sequences.

codon has evolved under a conserved model to the probability that a codon has evolved under a neutral model. The conserved model allows a codon to have evolved under negative selection and the neutral model assumes the rates of nonsynonymous and synonymous mutations are not significantly different. PolyPhen-2 uses both sequence- and structure-based predictive features to characterize the functional importance of a mutation, making use of non-redundant protein databases. SIFT is based on the principles of protein evolution and has been applied to a variety of organisms ranging from bacteria to humans. The algorithm is based on sequence homology and uses a median conservation score to measure protein conservation. The numbers of deleterious amino acid predictions for each strain are listed in Table 4 and predicted scores are provided in Additional file 10. The intersections of these predictions for SNPs that are polymorphic between LG/J and SM/J are illustrated in Figure 2. It is worth noting that the three different methods give largely non-overlapping results, which is consistent with a similar analysis using human genomes [73]. This result implies that our ability to reliably annotate whole genome sequences is still somewhat lacking.

In addition to SIFT predictions, VEP identifies variants falling in noncoding and potentially regulatory regions that may impact a gene's expression. An overview of potentially functional regulatory variants is listed in Table 4 and positions and scores are provided in Additional files 11 and 12.

LG/J, SM/J identical by descent regions

We identified genomic regions that are highly conserved between LG/J and SM/J using a hidden Markov model (Figure 1 and Additional file 13). These regions are defined as stretches of sequenced DNA ≥ 50 kbp in length containing little to no polymorphism between the strains. These regions are likely to be identical by descent (IBD), and are non-randomly distributed throughout the genome, being more clustered than expected by

chance ($p < 2.2e^{-16}$, Wald-Wolfowitz test). We classified 39% of the LG/J and SM/J sequenced genomes as IBD.

LG x SM QTL and whole-genome sequences

We integrated all of these data – IBD regions, polymorphisms and functional predictions – with 272 published QTL for metabolic traits (obesity, diabetes and serum-lipids) and for bone-growth traits (femur, humerus, radius and tibia length) mapped in very advanced intercrosses of LGxSM [37,48-51]. LOD scores range from 2.4 to 11.89 and are significant for their respective study. Additional file 14 describes these QTL, including their genomic coordinates, and their integration with various sequence characterizations. Figure 1 illustrates these QTL in relation to the sequence parameters we have generated. We find that 27% of all QTL interrogated in this study are covered by IBD bases, whereas 39% would be expected if they were randomly distributed. We find that both trait-specific QTL peaks (the point of the QTL with the lowest probability of a chance association with a specific trait) and QTL-specific peaks (accounting for pleiotropy, where more than one trait maps to a locus) are over-represented in non-IBD regions ($\chi^2 = 42.6$, $df = 1$, $p = 6.6 \times 10^{-11}$ for trait-specific peaks and $\chi^2 = 16.8$, $df = 1$, $p = 4.03 \times 10^{-05}$ for QTL-specific peaks). Further, we find that QTL regions are more likely to harbor variants that are predicted to have a functional impact by comparing the number of amino-acid changing variants predicted to be damaging by at least one algorithm and the number of variants predicted to fall in high-impact positions of transcription factor binding sites to empirical distributions of numbers generated from 1000 sets of randomly chosen non-QTL, non-IBD regions of similar size ($p < 2.2e^{-16}$ for both amino acid changing and TFBS variants, Additional file 15).

Integrating these data provides an opportunity to examine variation between LG/J and SM/J from both bottom-up (genomic sequence to phenotype) and top-down (phenotype to genomic sequence) perspectives with the goal of identifying plausible quantitative trait nucleotides (QTN) for testing mechanistic hypotheses. To illustrate a bottom-up approach, we focus on a SNP identified in the SM/J strain (chr13:104,041,257 A→C) falling in a cMyb TFBS (JASPAR ID MA01001) with a predicted high-impact (Figure 3). This position overlaps regulatory elements including H3K36 and H3K4 histone marks and a DNase1 hypersensitive site (ENSMUSR00000276453). The SNP falls in an intronic region of the oligopeptidase

Table 2 Genomic overview of structural variants

Variant	LG/J	SM/J	Polymorphic*
Deletion	7,697	9,889	11,206
Insertion	5,038	5,590	7,698
Inversion	94	159	184

*Refers to polymorphisms between LG/J and SM/J.

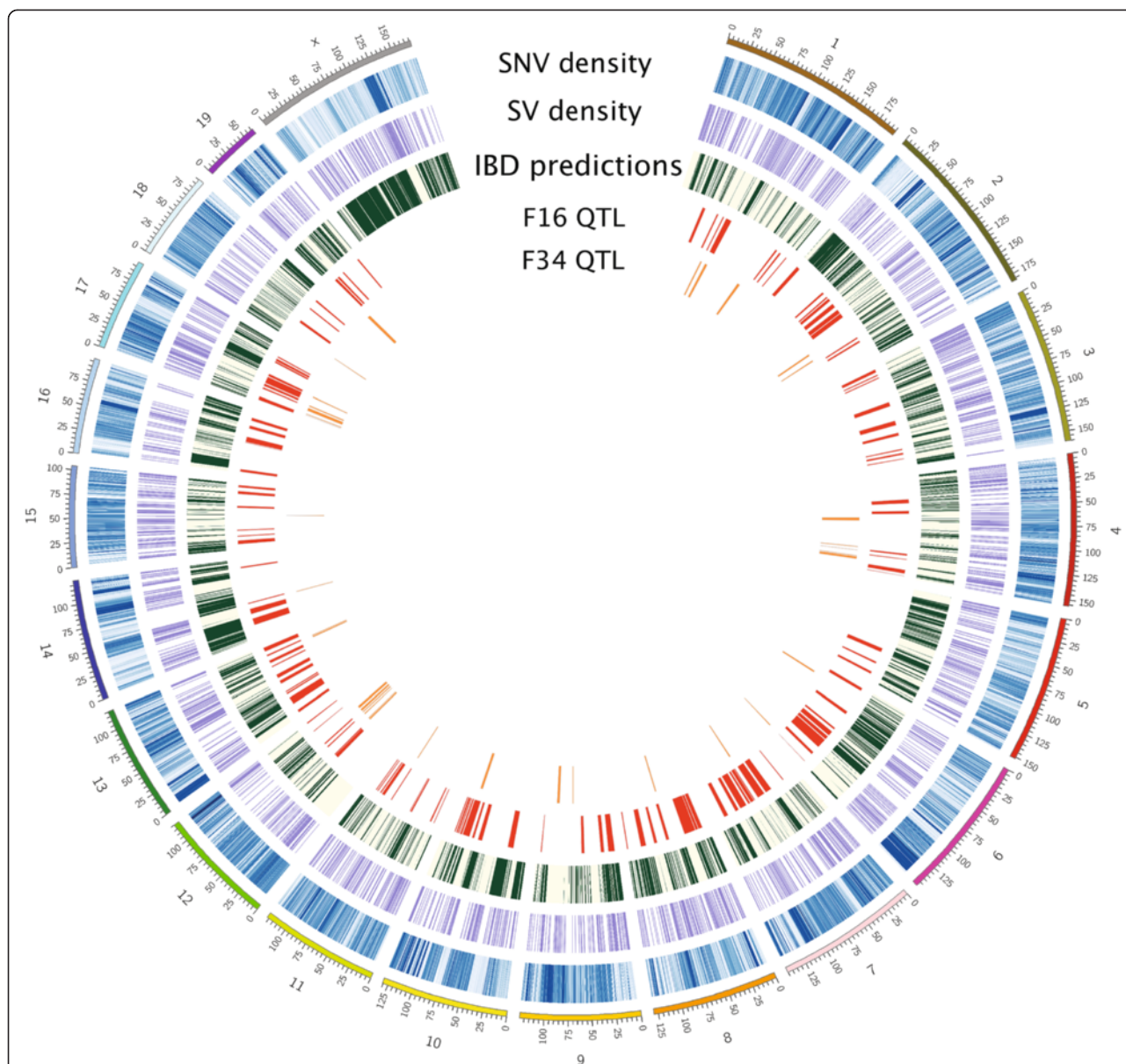


Figure 1 Circos plot illustrating the integration of polymorphic SNVs, SVs, and regions that are predicted to be identical-by-descent (i.e. harboring little to no variation) between the LG/J and SM/J inbred strains. These data are combined with QTL for metabolic traits mapped in an F₁₆ advanced intercross between LG/J and SM/J and with QTL for bone-growth traits mapped in an F₃₄ advanced intercross between these two strains.

Table 3 Comparison of high-coverage SNPs to low-coverage sequence in dbSNP

	LG/J	SM/J
Number of matched positions and variants	3,693,085	3,798,743
Number of mismatched variants at matched positions	20,266	44,582
Number of SNPs in dbSNP not called in high coverage genomes	411,859	391,672
New SNP variants identified in high coverage sequence	942,372	941,383

neurolysin, *Nln* (NM_029447). *Nln* knockout mice have been shown to be more insulin sensitive and glucose tolerant and to have increased gluconeogenesis relative to littermate controls [77]. In mammals, the liver is the main site of gluconeogenesis. A microarray analysis of hepatic gene expression shows *Nln* to be highly significantly differentially expressed between LG/J and SM/J, with the SM/J strain's expression barely detectable [78]. This gene falls within the support intervals of a QTL associated with basal serum glucose levels in an F₁₆ generation of an advanced intercross (AI) between the LG/J and SM/J strains [50]. Thus *Nln* is an attractive candidate quantitative trait

Table 4 Variants of predicted functional importance

	LRT	PolyPhen2	SIFT	Highly Informative TFBS (SNPs)	Highly Informative TFBS (Indels)
LG/J	800	2,748	2,198	578	61
SM/J	928	2,907	2,271	629	60
Polymorphic*	950	3,353	2,691	662	90

*Refers to polymorphisms between LG/J and SM/J.

gene (QTG) and this SNP is an attractive quantitative trait nucleotide (QTN) for further mechanistic studies of *Nln* involvement in glucose metabolism.

To illustrate a top-down approach, we focus on a QTL mapped in an F₃₄ generation of the LGxSM AI that is associated with variation in tibia length at chr6: 20,650,821-23,746,386 (Figure 4). There are 12 protein coding genes and 10 RNA genes falling within the QTL support interval [37]. Two of these genes, *Wnt16* (NM_053116) and *Ptprz1* (NM_001081306), are involved in limb development and/or bone formation [79,80]. Variants in a third gene, *Cped1* (NM_001081351), have recently been associated with variation in bone mineral density in a GWAS [81]. 23% of this QTL is covered by bases falling in IBD regions, but these three genes are located in non-IBD portions of the QTL. Three nonsynonymous SNPs fall in *Cped1* and are predicted to have functional consequences by at least one of the algorithms used: LRT, PolyPhen or SIFT. A fourth nonsynonymous SNP is predicted to have functional consequences by all three algorithms making it a highly attractive QTN. The SNP falls in exon 14 of *Ptprz1* (ENSMUSE00000619494, position 23016230 C→A; P1676H). This exon is highly conserved. Sanger sequencing confirmed the SM/J variant and the amino acid changing polymorphism between the strains. *Ptprz1* encodes the protein R-PTP-Z, which is thought to modulate osteoblast metabolism through

dephosphorylating *Src*, which plays a key role in osteoblast activities such as adhesion and differentiation [82,83]. The amino acid change occurs in the SM/J strain, and the only other strain of sequenced mouse carrying this variant is NZO/HILtJ. NZO/HILtJ is a common laboratory strain used as a model of metabolic syndrome because of its extreme obesity and hyperglycemic phenotype [84]. It bears no special relationship with SM/J, despite sharing this particular variant and a similar metabolic phenotype on a high-fat diet.

Conclusions

Here we describe the whole-genome sequences for the LG/J and SM/J inbred mouse strains. LG/J and SM/J are frequently compared in QTL mapping studies because of their great phenotypic diversity, and because this diversity is normally distributed in intercrosses of these two strains. This makes LG x SM an ideal model system for studying the genetic architecture of normal variation in complex traits, because this most closely mimics that found in human populations, where most variation is the result of many interacting genes of individually small effects. Comparison with previous imputation methods using SNPs called from low-coverage sequence for LG/J and SM/J indicated that there were many unreported variants in these strains [51,85]. Our sequence provides higher resolution, which allows us to capture more of the genomic sequence variation found in these strains with greater certainty.

Because we are interested in identifying candidate variants for functional follow-up, our first order of business was to identify regions of the LG/J and SM/J genomes that do not vary between the strains. Identification of IBD genomic regions is a powerful way to narrow existing QTL support intervals, as the regions that do not vary between the strains are unlikely to cause variation in the mapped trait. Further, identification of IBD and non-IBD regions between two strains is a powerful tool for testing mechanistic hypotheses and for planning focused candidate gene studies [86]. We classified 39% of the LG/J and SM/J sequenced genomes as IBD, and we are able to use this classification to narrow QTL support intervals by orders of magnitude when eliminating stretches of DNA that contain little to no variation between the parental strains within QTL support intervals.

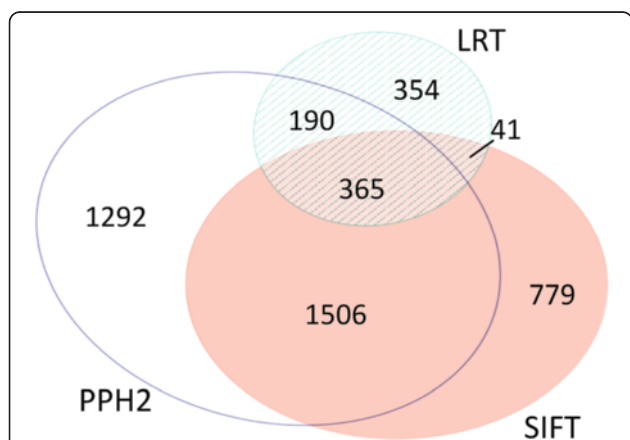
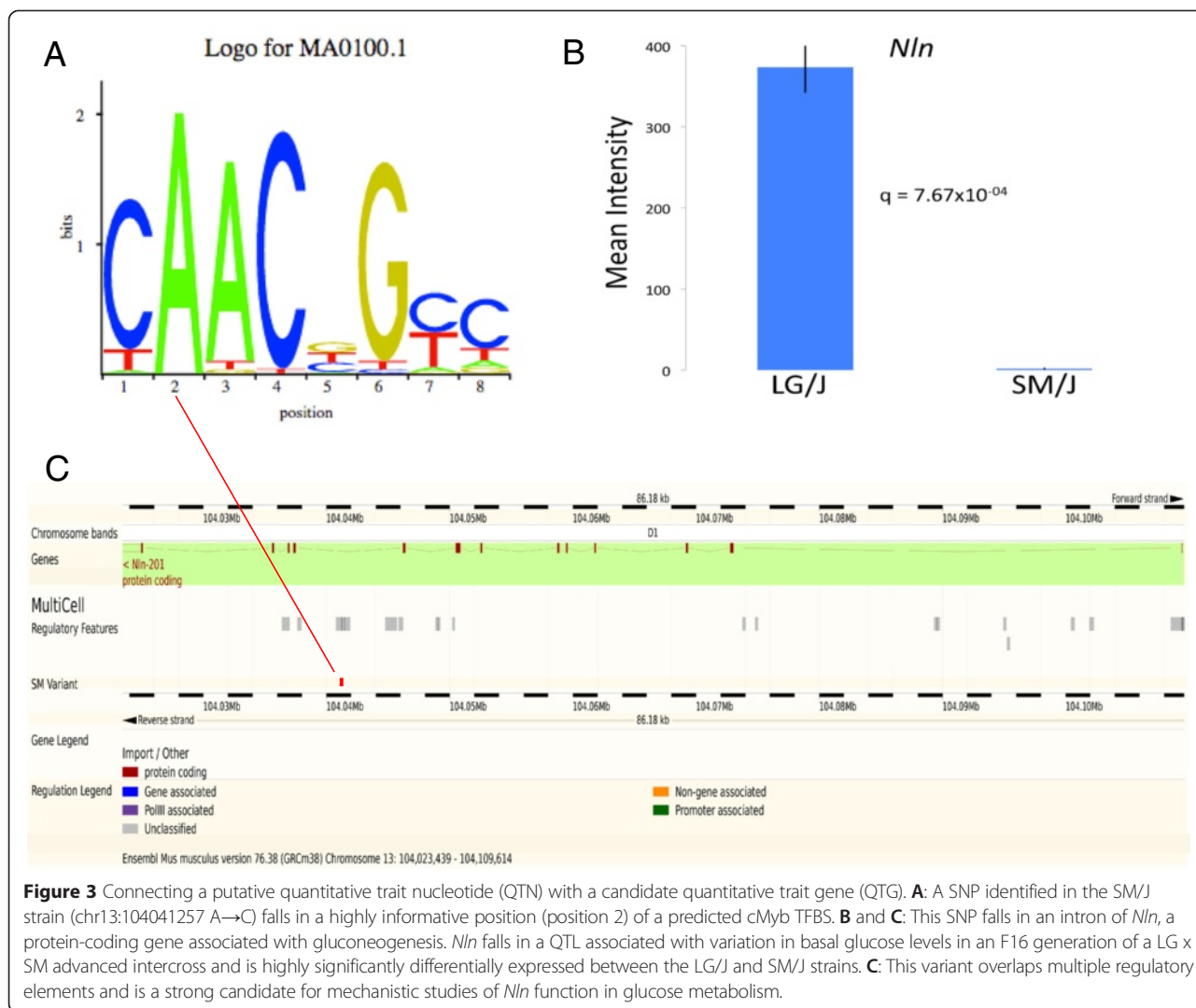


Figure 2 Proportional Venn diagram illustrating the intersections of three independent methods of predicting a functionally damaging amino acid changing SNP between the LG/J and SM/J strains.



Eliminating these regions does not explicitly rule them out as harboring potentially causal variants, however focusing on the non-IBD sequence within QTL support intervals – especially on the variants predicted to have functional consequences – allows one to prioritize the so-called ‘low-hanging fruit’. Other commonly used strain pairs, such as C57BL/6J and DBA/2J, have been sequenced but have not been subject to such close evaluation of IBD genomic regions within QTL.

We integrated the rich source of QTL results generated by very advanced intercrosses of LG x SM for metabolic traits (231 QTL associated with variation in obesity, diabetes and serum-lipids) mapped in the F₁₆ and for bone-growth traits (41 QTL associated with variation in femur, humerus, radius and tibia) mapped in the F₃₄ generations with the LG/J and SM/J genomic sequences. The median QTL interval in the F₁₆ data is ≈ 3.5mB and for the F₃₄ it is ≈ 2.0mB (Additional file 14). We find that ≈ 29% of F₁₆ and ≈ 19% of F₃₄ QTL intervals are covered by IBD

regions. Subtracting these IBD regions from QTL reduces the genomic search space for both generations, resulting in a comparable ≈ 1.2mB median number of per QTL bases for both F₁₆ and F₃₄ generations. We find that QTL from both generations have proportionally equivalent numbers of SNVs, bases covered by SVs, and bases predicted to have functional consequences (Additional file 14). Further, we find that QTL regions as a class are more likely to harbor variants predicted to have functional consequences relative to randomly selected non-QTL and non-IBD genomic regions of similar size (Additional file 15).

The traits associated with the QTL interrogated here belong to different classes of quantitative phenotype, namely metabolic traits mapped in the F₁₆ generation and developmental traits mapped in the F₃₄ generation. Having QTL for the same trait replicate in multiple generations of a mapping study increases the probability that the QTL is causal. However, given the high costs (both financial and time-wise) of breeding and maintaining large populations

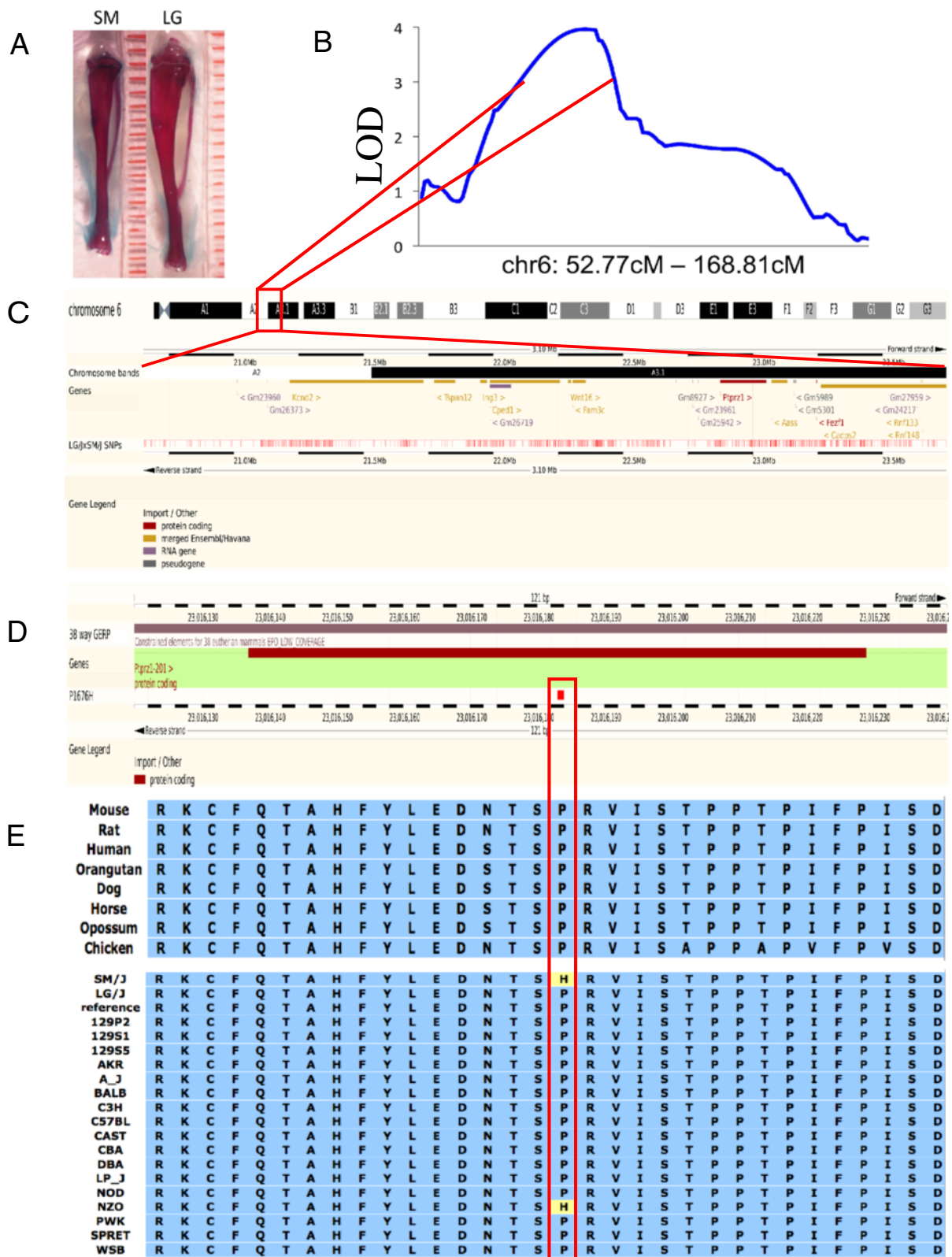


Figure 4 (See legend on next page.)

(See figure on previous page.)

Figure 4 Connecting phenotypic variation (QTL) to a candidate quantitative trait gene (QTG) and putative quantitative trait nucleotide (QTN). **A** and **B**: Variation in tibia length (mm) between LG and SM mapped to a QTL on chromosome 6. **C**: This QTL was localized to a genomic region and intersected with LG/J, SM/J SNPs and IBD regions. **D**: SNPs falling in non-IBD regions were interrogated and a SNP falling in exon 14 of *Ptprz1*, which affects bone-growth, was identified. The SNP changes the encoded amino acid from proline to histidine. **E**: This amino acid is 100% IBD and the amino acid variant occurs in SM/J and one other unrelated strain of laboratory mouse, NZO/HILtJ. This SNP is predicted to be functionally damaging by the LRT, PolyPhen-2 and SIFT algorithms, and represents a fruitful candidate QTN for further functional follow-up.

of mice for many generations, incorporating whole-genome sequence parameters as we have illustrated here can be used to extract compelling information from QTL mapped in earlier generations of intercrosses, even when the support intervals span many mega-bases of sequence. Thus whole-genome sequence data should be made part of the toolkit used to inform the design, execution and follow-up of QTL mapping studies.

We have highlighted variants falling in a QTL on chromosome 13 associated with basal glucose levels and a QTL on chromosome 6 associated with tibia length (Figures 3 and 4) to illustrate how all of these data – whole genome sequence variants, IBD regions, QTL, and functional predictions – can be integrated with each other and with other public datasets to identify and prioritize QTG and QTN. Identifying such variants within QTL in mice can facilitate translational research for correlated traits in human studies, and potentially uncover genetic underpinnings of disease phenotypes [87,88]. Our initial description and analysis of the LG/J and SM/J whole genomes offers new data that can be used to address fundamental questions about the molecular nature of quantitative phenotypic variation in an important model system.

Methods

Ethics statement

All animal care and handling procedures conformed to IACUC guidelines.

DNA isolation and library construction

DNA was isolated from the livers of one adult female LG/J and one adult female SM/J mouse using the Qiagen DNAeasy Blood and Tissue kit (Qiagen, West Sussex, UK). Genomic DNA was sonicated to an average size of 175 bp. The fragments were blunt ended, had addition of “A” base to 3’ end, and had Illumina’s sequencing adapters ligated to the ends. The ligated fragments underwent amplification incorporating a unique indexing sequence tag. The resulting libraries were sequenced on 6 lanes using the Illumina HiSeq-2500 as paired end reads extending 101 bases from both ends of the fragments.

Alignment and SNP detection

Reads were aligned to the GRC m38 (mm10) mouse reference genome using NovoAlign-2.08.02 and a BAM file was produced for each strain (<http://www.novocraft.com>).

The gene annotation model used was Ensembl *Mus musculus* GRC 38.72. Variants were called from each strain’s BAM file using two variant discovery tools: SAMtools pileup and FreeBayes Bayesian genetic variant detector [89,90]. Results were merged and only variants with a minimum read depth of 3 and a quality score of at least 20 for SNPs and at least 50 for indels were included in the final set of SNVs for analysis.

Quality assessment and Sanger sequencing candidate variant

SNPs identified for LG/J and SM/J were compared to SNPs called from independently generated, low-coverage sequence available on dbSNP [91] using custom python scripts. DNA was isolated from the livers of 4 female LG/J and 4 female SM/J animals to validate the candidate amino acid changing mutation P1676H in exon 14 of *Ptprz1*. The following primers were designed: Forward 5’-GCT CCA TGG CCA CTA TCT TTA CTC-3’ and reverse 5’-CAA TTC ATG CCT CAA GGT GAC TGC-3’. Sanger sequencing was performed by Genewiz (South Plainfield, NJ).

Comparison with variants identified in other sequenced mouse strains

VCF files for SNPs discovered in 18 mouse strains’ whole-genomes were downloaded (<http://www.sanger.ac.uk/resources/mouse/genomes>) and compared to LG/J and SM/J SNPs using custom python scripts.

Structural variant prediction

Structural variants (SV) were identified using a local implementation of the SVmerge pipeline [92]. SVmerge simplifies SV discovery and integration using multiple SV discovery algorithms, producing a single consensus SV callset. The SVmerge pipeline was run with 4 calling algorithms: Breakdancer 1.0, pindel 0.2.4q, SECluster and cnD [92-95]. After merging the results of these 4 callers into a single consensus callset, the Velvet genome assembler was used to attempt breakpoint assembly for all SVs in the callset [96].

Deleterious mutation prediction

LRT

Deleterious amino-acid changing mutations were predicted using a likelihood ratio test (LRT) as described in

Chun and Fay (2009). The algorithm was modified to compare the genomes of LG/J and SM/J each to the reference C57BL/6 J. P-values were calculated by comparing twice the log-likelihood ratio of the two models to a χ^2 distribution with $df = 1$. Deleterious amino acid changing mutations were predicted using an LRT cutoff of $p < 0.001$ while controlling for false positives and false negatives as previously described and modified for mouse genomic sequence [73].

PolyPhen-2

PolyPhen-2 was downloaded and run locally to predict deleterious mutations in the LG/J and SM/J genomes. The algorithm supports analysis of mouse proteins using prebuilt human models if the option '-n mouse' is specified when preparing the local copy of UniProtKB (www.uniprot.org). Deleterious amino acid changing mutations were predicted for both strains using a recommended false discovery rate (FDR) cutoff of 20% [74].

VEP and SIFT

VEP was downloaded and run locally to predict deleterious mutations in the LG/J and SM/J genomes using alignments built using the TrEMBL 39.8 protein database. Deleterious amino acid changing mutations were predicted for both strains using a score of < 0.05 and a median conservation cutoff of 3.25. Regulatory annotations are based on the Ensembl regulatory build, which integrates data from ENCODE and several other large scale projects. Transcription factor binding site (TFBS) variant scoring is provided for regulatory regions that have ChIP-seq data to support binding predictions. This is done using the MOODS software [97], which assigns significance scores by matching polymorphisms against motifs in the JASPAR database [98]. The output was filtered for TFBS sites that are classified as 'Highly Informative' by the software.

IBD region identification

To identify regions of shared ancestral background, we clustered segments of observed polymorphisms using a two state hidden Markov model. For each state, we modeled two types of observations: 1) the number of polymorphisms in a 50kbp window; and 2) the observation of a SV in a 50kbp window. The count of polymorphisms is expressed as a Poisson variable, while the occurrence of a SV is a Binomial variable. Parameters for this model were estimated using the EM algorithm implemented in the depmixS4 package in the R programming language [99]. A Wald-Wolfowitz test of randomness was performed using the adehabitatLT package in R [100].

Data integration

The QTL interrogated in this study are from previously published studies that mapped to the mm9 (NCBI build

37) mouse reference genome. QTL peaks and support intervals were converted to mm10 (GRC m38) using the Batch Coordinate Conversion (liftOver) tool [101]. Sequence data and results generated here were integrated with other published and publically available data as indicated using custom python and R scripts.

Data access

We have made these data available to the community through multiple data portals: LG/J (SAMN03075510) and SM/J (SAMN03075514) raw reads have been submitted to the NCBI Sequence Read Archive and BAM files have been submitted to the Wellcome Trust mouse genomes portal (<http://www.sanger.ac.uk/resources/mouse/genomes>). Other results from this study are available as Additional files 1, 2, 3, 4, 5, 6, 7, 8, 9, 10, 11, 12, 13, 14, and 15.

Additional files

- Additional file 1:** LG/J, SM/J and LG/J x SM/J polymorphic SNPs overview.
- Additional file 2:** LG/J, SM/J and LG/J x SM/J polymorphic indels overview.
- Additional file 3:** SNPs in LG/J discovered by integrating output from SamTools pileup and FreeBayes variant discovery tools.
- Additional file 4:** Indels in LG/J discovered by integrating output from SamTools pileup and FreeBayes variant discovery tools.
- Additional file 5:** SNPs in SM/J discovered by integrating output from SamTools pileup and FreeBayes variant discovery tools.
- Additional file 6:** Indels in SM/J discovered by integrating output from SamTools pileup and FreeBayes variant discovery tools.
- Additional file 7:** Structural variants found in LG/J and SM/J.
- Additional file 8:** Distances between the LG/J and SM/J strains and other sequenced strains.
- Additional file 9:** Phylogenetic tree of 20 sequenced mouse strains.
- Additional file 10:** Amino acid changing mutations and corresponding deleterious predicted scores using SIFT/polyphen/LRT for both LG/J and SM/J strains.
- Additional file 11:** VEP output of variants in predicted regulatory features for both LG/J and SM/J.
- Additional file 12:** VEP output of variants in predicted motifs for both LG/J and SM/J.
- Additional file 13:** Predicted IBD regions in LG/J and SM/J sequenced genomes.
- Additional file 14:** QTL metrics and sequence integration.
- Additional file 15:** Distribution of the number of variants predicted to have functional consequences in QTL intervals and in 1000 sets of randomly selected non-QTL regions of similar size.

Abbreviations

SNVs: Small nucleotide variants; SVs: Structural variants; IBD: Identical-by-descent; TFBS: Transcription factor binding sites; QTL: Quantitative trait loci; candidate QTG: Quantitative trait gene; QTN: Quantitative trait nucleotide; SNPs: Single nucleotide polymorphisms; Indels: Insertion-deletions; LRT: Likelihood ratio test; FDR: False discovery rate.

Competing interests

The authors declare that they have no competing interests.

Authors' contributions

IN, DC, SC, JF, and HL generated and analyzed data. JC and HL wrote the manuscript. All authors edited and approved the final manuscript.

Acknowledgements

This work was supported by NIH-NIDDK K01 DK095003 and P30 DK056341 to HAL and in part by NIMH R01MH10180 to DFC and by NIH-NCRRL UL1 RR024992 to the genome technology access center at Washington university in St Louis. The content of this paper is solely the responsibility of the authors and does not necessarily represent the official views of the national institutes of health.

Author details

¹Department of Genetics, Washington University School of Medicine, Campus Box 8108 660 S Euclid Ave, St Louis, MO 63110, USA. ²Division of Genetics, Brigham and Women's Hospital and Harvard Medical School, Boston, MA, USA. ³Department of Biology, Loyola University, Chicago, IL, USA.

Received: 28 October 2014 Accepted: 28 April 2015

Published online: 28 May 2015

References

- Beck JA, Lloyd S, Hafezparast M, Lennon-Pierce M, Eppig JT, Festing MF, et al. Genealogies of mouse inbred strains. *Nat Genet.* 2000;24(1):23–5.
- Goodale HD. A study of the inheritance of body weight in the albino mouse by selection. *J Hered.* 1938;29:101–12.
- Wilson SP, Goodale HD, Kyle WH, Godfrey EF. Long term selection for body weight in mice. *The Journal of Heredity.* 1971;62:228–34.
- MacArthur JW. Genetics of body size and related characters. I. Selecting small and large races of the laboratory mouse. *Am Nat.* 1944;78(775):142–57.
- Hrbek T, de Brito RA, Wang B, Pletscher LS, Cheverud JM. Genetic characterization of a new set of recombinant inbred lines (LGXSM) formed from the inter-cross of SM/J and LG/J inbred mouse strains. *Mamm Genome.* 2006;17(5):417–29.
- Chai CK. Analysis of quantitative inheritance of body size in mice. I: hybridization and maternal influence. *Genetics.* 1956;41:157–64.
- Chai CK. Analysis of quantitative inheritance of body size in mice. III. Dominance. *Genetics.* 1957;42(5):601–7.
- Chai CK. Analysis of quantitative inheritance of body size in mice. II: gene action and segregation. *Genetics.* 1956;41:167–78.
- Chai CK. Analysis of quantitative inheritance of body size in mice. IV. An attempt to isolate polygenes. *Genet Res.* 1961;2:25–32.
- Chai CK. Analysis of quantitative inheritance of body size in mice. V. Effects of small numbers of polygenes on similar genetic backgrounds. *Genet Res.* 1968;11(3):239–46.
- Cheverud JM, Routman EJ, Duarte FA, van Swinderen B, Cothran K, Perel C. Quantitative trait loci for murine growth. *Genetics.* 1996;142(4):1305–19.
- Vaughn TT, Pletscher LS, Peripato A, King-Ellison K, Adams E, Erikson C, et al. Mapping quantitative trait loci for murine growth: a closer look at genetic architecture. *Genet Res.* 1999;74(3):313–22.
- Wu R, Wang Z, Zhao W, Cheverud JM. A mechanistic model for genetic machinery of ontogenetic growth. *Genetics.* 2004;168(4):2383–94.
- Zhao W, Ma C, Cheverud JM, Wu R. A unifying statistical model for QTL mapping of genotype x sex interaction for developmental trajectories. *Physiol Genomics.* 2004;19(2):218–27.
- Lin M, Ma CX, Zhao W, Cheverud JM, Wu R. Mechanistic mapping of ontogenetic growth based on biological principles. *Growth Dev Aging.* 2005;69(1):31–7.
- Zhao W, Chen YQ, Casella G, Cheverud JM, Wu R. A non-stationary model for functional mapping of complex traits. *Bioinformatics.* 2005;21(10):2469–77.
- Long F, Chen YQ, Cheverud JM, Wu R. Genetic mapping of allometric scaling laws. *Genet Res.* 2006;87(3):207–16.
- Hager R, Cheverud JM, Wolf JB. Relative contribution of additive, dominance, and imprinting effects to phenotypic variation in body size and growth between divergent selection lines of mice. *Evolution.* 2009;63(5):1118–28.
- Kramer M, Vaughn TC, Pletscher LS, King-Ellison K, Adams E, Erikson C, et al. Genetic variation in body weight growth and composition in the intercross of large (LG/J) and small (SM/J) inbred strains of mice. *Genet Mol Biol.* 1998;21:211–8.
- Leamy LJ, Routman E, Cheverud J. Quantitative trait loci for early and late developing skull characters in mice: a test of the genetic independence model of morphological integration. *Am Nat.* 1999;153:201–14.
- Wolf JB, Leamy LJ, Routman EJ, Cheverud JM. Epistatic pleiotropy and the genetic architecture of covariation within early and late-developing skull trait complexes in mice. *Genetics.* 2005;171(2):683–94.
- Roseman C, Kenney-Hunt J, Cheverud J. Phenotypic integration without modularity: testing hypotheses about the distribution of pleiotropic quantitative trait loci in a continuous space. *Evol Biol.* 2009;36:282–91.
- Cheverud J, Routman E, Irschick D. Pleiotropic effects of individual gene loci on mandibular morphology. *Evolution.* 1997;51:2004–14.
- Cheverud JM, Ehrich TH, Vaughn TT, Koreishi SF, Linsey RB, Pletscher LS. Pleiotropic effects on mandibular morphology II: differential epistasis and genetic variation in morphological integration. *J Exp Zool B Mol Dev Evol.* 2004;302(5):424–35.
- Klingenberg CP, Leamy LJ, Routman EJ, Cheverud JM. Genetic architecture of mandible shape in mice: effects of quantitative trait loci analyzed by geometric morphometrics. *Genetics.* 2001;157(2):785–802.
- Ehrich TH, Vaughn TT, Koreishi SF, Linsey RB, Pletscher LS, Cheverud JM. Pleiotropic effects on mandibular morphology I. Developmental morphological integration and differential dominance. *J Exp Zool B Mol Dev Evol.* 2003;296(1):58–79.
- Leamy LJ, Pomp D, Eisen EJ, Cheverud JM. Quantitative trait loci for directional but not fluctuating asymmetry of mandible characters in mice. *Genet Res.* 2000;76(1):27–40.
- Leamy LJ, Pomp D, Eisen EJ, Cheverud JM. Pleiotropy of quantitative trait loci for organ weights and limb bone lengths in mice. *Physiol Genomics.* 2002;10(1):21–9.
- Leamy LJ, Klingenberg CP, Sherratt E, Wolf JB, Cheverud JM. A search for quantitative trait loci exhibiting imprinting effects on mouse mandible size and shape. *Heredity (Edinb).* 2008;101(6):518–26.
- Willmore KE, Roseman CC, Rogers J, Cheverud JM, Richtsmeier JT. Comparison of mandibular phenotypic and genetic integration between baboon and mouse. *Evol Biol.* 2009;36(1):19–36.
- Workman MS, Leamy LJ, Routman EJ, Cheverud JM. Analysis of quantitative trait locus effects on the size and shape of mandibular molars in mice. *Genetics.* 2002;160(4):1573–86.
- Leamy LJ, Workman MS, Routman EJ, Cheverud JM. An epistatic genetic basis for fluctuating asymmetry of tooth size and shape in mice. *Heredity (Edinb).* 2005;94(3):316–25.
- Kenney-Hunt JP, Vaughn TT, Pletscher LS, Peripato A, Routman E, Cothran K, et al. Quantitative trait loci for body size components in mice. *Mamm Genome.* 2006;17(6):526–37.
- Norgard EA, Roseman CC, Fawcett GL, Pavlicev M, Morgan CD, Pletscher LS, et al. Identification of quantitative trait loci affecting murine long bone length in a two-generation intercross of LG/J and SM/J mice. *J Bone Miner Res.* 2008;23(6):887–95.
- Pavlicev M, Kenney-Hunt JP, Norgard EA, Roseman CC, Wolf JB, Cheverud JM. Genetic variation in pleiotropy: differential epistasis as a source of variation in the allometric relationship between long bone lengths and body weight. *Evolution.* 2008;62(1):199–213.
- Norgard EA, Jarvis JP, Roseman CC, Maxwell TJ, Kenney-Hunt JP, Samochoa KE, et al. Replication of long-bone length QTL in the F9–F10 LG, SM advanced intercross. *Mamm Genome.* 2009;20(4):224–35.
- Norgard EA, Lawson HA, Pletscher LS, Wang B, Brooks VR, Wolf JB, et al. Genetic factors and diet affect long-bone length in the F34 LG, SM advanced intercross. *Mamm Genome.* 2011;22(3–4):178–96.
- Reich MS, Jarvis JP, Silva MJ, Cheverud JM. Genetic relationships between obesity and osteoporosis in LGXSM recombinant inbred mice. *Genet Res (Camb).* 2008;90(5):433–44.
- Carson EA, Kenney-Hunt JP, Pavlicev M, Bouckaert KA, Chinn AJ, Silva MJ, et al. Weak genetic relationship between trabecular bone morphology and obesity in mice. *Bone.* 2012;51(1):46–53.
- Cheverud JM, Vaughn TT, Pletscher LS, Peripato AC, Adams ES, Erikson CF, et al. Genetic architecture of adiposity in the cross of LG/J and SM/J inbred mice. *Mamm Genome.* 2001;12(1):3–12.
- Cheverud JM, Ehrich TH, Hrbek T, Kenney JP, Pletscher LS, Semenkovich CF. Quantitative trait loci for obesity- and diabetes-related traits and their dietary responses to high-fat feeding in LGXSM recombinant inbred mouse strains. *Diabetes.* 2004;53(12):3328–36.
- Cheverud JM, Ehrich TH, Kenney JP, Pletscher LS, Semenkovich CF. Genetic evidence for discordance between obesity- and diabetes-related

- traits in the LGXSM recombinant inbred mouse strains. *Diabetes*. 2004;53(10):2700–8.
43. Fawcett GL, Roseman CC, Jarvis JP, Wang B, Wolf JB, Cheverud JM. Genetic architecture of adiposity and organ weight using combined generation QTL analysis. *Obesity* (Silver Spring). 2008;16(8):1861–8.
 44. Fawcett GL, Jarvis JP, Roseman CC, Wang B, Wolf JB, Cheverud JM. Fine-mapping of obesity-related quantitative trait loci in an F9/10 advanced intercross line. *Obesity* (Silver Spring). 2010;18(7):1383–92.
 45. Parker CC, Cheng R, Sokoloff G, Lim JE, Skol AD, Abney M, et al. Fine-mapping alleles for body weight in LG/J x SM/J F and F(34) advanced intercross lines. *Mamm Genome*. 2011;22(9–10):563–71.
 46. Ehrich TH, Kenney JP, Vaughn TT, Pletscher LS, Cheverud JM. Diet, obesity, and hyperglycemia in LG/J and SM/J mice. *Obes Res*. 2003;11(11):1400–10.
 47. Ehrich TH, Kenney-Hunt JP, Pletscher LS, Cheverud JM. Genetic variation and correlation of dietary response in an advanced intercross mouse line produced from two divergent growth lines. *Genet Res*. 2005;85(3):211–22.
 48. Cheverud JM, Lawson HA, Fawcett GL, Wang B, Pletscher LS ARF, Maxwell TJ, et al. Diet-dependent genetic and genomic imprinting effects on obesity in mice. *Obesity* (Silver Spring). 2011;19(1):160–70.
 49. Lawson HA, Zelle KM, Fawcett GL, Wang B, Pletscher LS, Maxwell TJ, et al. Genetic, epigenetic, and gene-by-diet interaction effects underlie variation in serum lipids in a LG/JxSM/J murine model. *J Lipid Res*. 2010;51(10):2976–84.
 50. Lawson HA, Lee A, Fawcett GL, Wang B, Pletscher LS, Maxwell TJ, et al. The importance of context to the genetic architecture of diabetes-related traits is revealed in a genome-wide scan of a LG/J x SM/J murine model. *Mamm Genome*. 2011;22(3–4):197–208.
 51. Lawson HA, Cady JE, Partridge C, Wolf JB, Semenkovich CF, Cheverud JM. Genetic effects at pleiotropic loci are context-dependent with consequences for the maintenance of genetic variation in populations. *PLoS Genet*. 2011;7(9), e1002256.
 52. Jarvis JP, Kenney-Hunt J, Ehrich TH, Pletscher LS, Semenkovich CF, Cheverud JM. Maternal genotype affects adult offspring lipid, obesity, and diabetes phenotypes in LGXSM recombinant inbred strains. *J Lipid Res*. 2005;46(8):1692–702.
 53. Hager R, Cheverud JM, Wolf JB. Maternal effects as the cause of parent-of-origin effects that mimic genomic imprinting. *Genetics*. 2008;178(3):1755–62.
 54. Wolf JB, Vaughn TT, Pletscher LS, Cheverud JM. Contribution of maternal effect QTL to genetic architecture of early growth in mice. *Heredity* (Edinb). 2002;89(4):300–10.
 55. Wolf JB, Leamy LJ, Roseman CC, Cheverud JM. Disentangling prenatal and postnatal maternal genetic effects reveals persistent prenatal effects on offspring growth in mice. *Genetics*. 2011;189(3):1069–82.
 56. Wolf J, Cheverud JM. Detecting maternal-effect Loci by statistical cross-fostering. *Genetics*. 2012;191(1):261–77.
 57. Wolf JB, Cheverud JM, Roseman C, Hager R. Genome-wide analysis reveals a complex pattern of genomic imprinting in mice. *PLoS Genet*. 2008;4(6), e1000091.
 58. Cheverud JM, Lawson HA, Funk R, Zhou J, Blankenhorn EP, Heber-Katz E. Healing quantitative trait loci in a combined cross analysis using related mouse strain crosses. *Heredity* (Edinb). 2012;108(4):441–6.
 59. Cheverud JM, Lawson HA, Bouckaert K, Kossenkov AV, Showe LC, Cort L, et al. Fine-mapping quantitative trait loci affecting murine external ear tissue regeneration in the LG/J by SM/J advanced intercross line. *Heredity* (Edinb). 2014;112:508–18.
 60. Blankenhorn EP, Bryan G, Kossenkov AV, Clark LD, Zhang XM, Chang C, et al. Genetic loci that regulate healing and regeneration in LG/J and SM/J mice. *Mamm Genome*. 2009;20(11–12):720–33.
 61. Bedelbaeva K, Snyder A, Gourevitch D, Clark L, Zhang XM, Leferovich J, et al. Lack of p21 expression links cell cycle control and appendage regeneration in mice. *Proc Natl Acad Sci U S A*. 2010;107(13):5845–50.
 62. Rai MF, Hashimoto S, Johnson EE, Janiszak KL, Fitzgerald J, Heber-Katz E, et al. Heritability of articular cartilage regeneration and its association with ear-wound healing. *Arthritis Rheum*. 2012;64:2300–10.
 63. Hashimoto S, Rai MF, Janiszak KL, Cheverud JM, Sandell LJ. Cartilage and bone changes during development of post-traumatic osteoarthritis in selected LGXSM recombinant inbred mice. *Osteoarthritis Cartilage*. 2012;20(6):562–71.
 64. Samochoa KE, Lim JE, Cheng R, Sokoloff G, Palmer AA. Fine mapping of QTL for prepulse inhibition in LG/J and SM/J mice using F(2) and advanced intercross lines. *Genes Brain Behav*. 2010;9(7):759–67.
 65. Cheng R, Lim JE, Samochoa KE, Sokoloff G, Abney M, Skol AD, et al. Genome-wide association studies and the problem of relatedness among advanced intercross lines and other highly recombinant populations. *Genetics*. 2010;185(3):1033–44.
 66. Bartnikas TB, Parker CC, Cheng R, Campagna DR, Lim JE, Palmer AA, et al. QTLs for murine red blood cell parameters in LG/J and SM/J F(2) and advanced intercross lines. *Mamm Genome*. 2012;23:356–66.
 67. Carroll AM, Palmer AA, Lionikas A. QTL analysis of type I and type IIA fibers in soleus muscle in a cross between LG/J and SM/J mouse strains. *Front Genet*. 2011;2:99.
 68. Lionikas A, Cheng R, Lim JE, Palmer AA, Blizard DA. Fine-mapping of muscle weight QTL in LG/J and SM/J intercrosses. *Physiol Genomics*. 2010;42A(1):33–8.
 69. Yalcin B, Wong K, Agam A, Goodson M, Keane TM, Gan X, et al. Sequence-based characterization of structural variation in the mouse genome. *Nature*. 2011;477(7364):326–9.
 70. Keane TM, Goodstadt L, Danecek P, White MA, Wong K, Yalcin B, et al. Mouse genomic variation and its effect on phenotypes and gene regulation. *Nature*. 2011;477(7364):289–94.
 71. Petkov PM, Graber JH, Churchill GA, DiPetrillo K, King BL, Paigen K. Evidence of a large-scale functional organization of mammalian chromosomes. *PLoS Genet*. 2005;1(3), e33.
 72. Eppig JT, Blake JA, Bult CJ, Kadin JA, Richardson JE, The_Mouse_Genome_Database_Group. The mouse genome database (MGD): comprehensive resource for genetics and genomics of the laboratory mouse. *Nucleic Acids Res*. 2012;40(1):881–6.
 73. Chun S, Fay JC. Identification of deleterious mutations within three human genomes. *Genome Res*. 2009;19(9):1553–61.
 74. Adzhubei IA, Schmidt S, Peshkin L, Ramensky VE, Gerasimova A, Bork P, et al. A method and server for predicting damaging missense mutations. *Nat Methods*. 2010;7(4):248–9.
 75. Kumar P, Henikoff S, Ng PC. Predicting the effects of coding non-synonymous variants on protein function using the SIFT algorithm. *Nat Protoc*. 2009;4(7):1073–81.
 76. McLaren W, Pritchard B, Rios D, Chen Y, Flicek P, Cunningham F. Deriving the consequences of genomic variants with the ensembl API and SNP effect predictor. *Bioinformatics*. 2010;26(16):2069–70.
 77. Cavalcanti DM, Castro LM, Rosa Neto JC, Seelaender M, Neves RX, Oliveira V, et al. Neurolysin knockout mice generation and initial phenotype characterization. *J Biol Chem*. 2014;289(22):15426–40.
 78. Partridge CG, Fawcett GL, Wang B, Semenkovich CF, Cheverud JM. The effect of dietary fat intake on hepatic gene expression in LG/J AND SM/J mice. *BMC Genomics*. 2014;15:99.
 79. Schinke T, Gebauer M, Schilling AF, Lamprianou S, Priemel M, Mueledner C, et al. The protein tyrosine phosphatase rtpzeta is expressed in differentiated osteoblasts and affects bone formation in mice. *Bone*. 2008;42(3):524–34.
 80. Witte F, Dokas J, Neuendorf F, Mundlos S, Stricker S. Comprehensive expression analysis of all Wnt genes and their major secreted antagonists during mouse limb development and cartilage differentiation. *Gene Expr Patterns*. 2009;9(4):215–23.
 81. Kemp JP, Medina-Gomez C, Estrada K, St Pourcain B, Heppner DH, Warrington NM, et al. Phenotypic dissection of bone mineral density reveals skeletal site specificity and facilitates the identification of novel loci in the genetic regulation of bone mass attainment. *PLoS Genet*. 2014;10(6), e1004423.
 82. Toledo SR, Oliveira ID, Okamoto OK, Zago MA, de Seixas Alves MT, Filho RJ, et al. Bone deposition, bone resorption, and osteosarcoma. *J Orthop Res*. 2010;28(9):1142–8.
 83. Zambuzzi WF, Milani R, Teti A. Expanding the role of Src and protein-tyrosine phosphatases balance in modulating osteoblast metabolism: lessons from mice. *Biochimie*. 2010;92(4):327–32.
 84. Bray GA, York DA. Genetically transmitted obesity in rodents. *Physiol Rev*. 1971;51(3):598–646.
 85. Wang JR, de Villena FP, Lawson HA, Cheverud JM, Churchill GA, McMillan L. Imputation of single-nucleotide polymorphisms in inbred mice using local phylogeny. *Genetics*. 2012;190(2):449–58.
 86. DiPetrillo K, Wang X, Stylianou IM, Paigen B. Bioinformatics toolbox for narrowing rodent quantitative trait loci. *Trends Genet*. 2005;21(12):683–92.
 87. Kraja AT, Lawson HA, Arnett DK, Borecki IB, Broeckel U, de Las Fuentes L, et al. Obesity-insulin targeted genes in the 3p26-25 region in human studies and LG/J and SM/J mice. *Metabolism*. 2012;61:1129–41.

88. Lawson HA. Animal models of metabolic syndrome. In: Conn M, editor. *Animal models of human disease*. Cambridge: Elsevier; 2013. p. 243–64. vol. 1.
89. Li H, Handsaker B, Wysoker A, Fennell T, Ruan J, Homer N, et al. The sequence alignment/Map format and SAMtools. *Bioinformatics*. 2009;25(16):2078–9.
90. Garrison E, Marth G. Haplotype-based variant detection from short-read sequencing. In: arXiv preprint arXiv:1207.3907[q-bio.GN]; 2012.
91. Sherry ST, Ward MH, Kholodov M, Baker J, Phan L, Smigielski EM, et al. dbSNP: the NCBI database of genetic variation. *Nucleic Acids Res*. 2001;29(1):308–11.
92. Wong K, Keane TM, Stalker J, Adams DJ. Enhanced structural variant and breakpoint detection using SVMerge by integration of multiple detection methods and local assembly. *Genome Biol*. 2010;11(12):R128.
93. Chen K, Wallis JW, McLellan MD, Larson DE, Kalicki JM, Pohl CS, et al. BreakDancer: an algorithm for high-resolution mapping of genomic structural variation. *Nat Methods*. 2009;6(9):677–81.
94. Ye K, Schulz MH, Long Q, Apweiler R, Ning Z. Pindel: a pattern growth approach to detect break points of large deletions and medium sized insertions from paired-end short reads. *Bioinformatics*. 2009;25(21):2865–71.
95. Simpson JT, McIntyre RE, Adams DJ, Durbin R. Copy number variant detection in inbred strains from short read sequence data. *Bioinformatics*. 2010;26(4):565–7.
96. Zerbino DR, Birney E. Velvet: algorithms for de novo short read assembly using de bruijn graphs. *Genome Res*. 2008;18(5):821–9.
97. Korhonen J, Martinmaki P, Pizzi C, Rastas P, Ukkonen E. MOODS: fast search for position weight matrix matches in DNA sequences. *Bioinformatics*. 2009;25(23):3181–2.
98. Bryne JC, Valen E, Tang MH, Marstrand T, Winther O, da Piedade I, et al. JASPAR, the open access database of transcription factor-binding profiles: new content and tools in the 2008 update. *Nucleic Acids Res*. 2008;36(Database issue):D102–106.
99. Visser: Depmix: An R-package for fitting mixture models on mixed multivariate data with Markov dependencies. In: R-package manual and introduction into Dependent Mixture models. 2007. [dssm.unipa.it/CRAN/web/packages/depmix/citation.html]
100. Calenge C. The package adehabitat for the R software: a tool for the analysis of space and habitat use by animals. *Ecol Model*. 2006;197:516–9.
101. Karolchik D, Barber GP, Casper J, Clawson H, Cline MS, Diekhans M, et al. The UCSC genome browser database: 2014 update. *Nucleic Acids Res*. 2014;42(Database issue):D764–770.

Submit your next manuscript to BioMed Central and take full advantage of:

- Convenient online submission
- Thorough peer review
- No space constraints or color figure charges
- Immediate publication on acceptance
- Inclusion in PubMed, CAS, Scopus and Google Scholar
- Research which is freely available for redistribution

Submit your manuscript at
www.biomedcentral.com/submit

